# A millisecond-risetime sub-millimeter light source for lab and in flight bolometer calibration.

Ph. Abbon, A. Delbart, M. Fesquet, C. Magneville, B. Mazeau, J-P. Pansart, D. Yvon [1],

*DAPNIA CEA Saclay, 91191 Gif/Yvette Cedex, France*

L. Dumoulin, S. Marnieros,

*IN2P3/CSNSM, Orsay, France*

Ph. Camus, T. Durand, Ch. Hoffmann,

*CEA/CRTBT, Grenoble, France*

**Abstract**

The Olimpo balloon project will use a 120 bolometer camera to observe the sky at 4 frequencies (143, 217, 385 and 600 $GHz$) with a resolution of 3 to 2 arc-minute. This paper presents the sub-millimeter calibration "lamp" developed for ground testing and in-flight secondary calibration of bolometric detectors. By design, main features of the device are reproductibility and stability of light flux and millisecond rise time. The radiative device will be placed inside the bolometer camera and will illuminate the bolometer array through a hole in the last 2 $K$ mirror. Operation, readout, and monitoring of the device is ensured by warm electronics. Light output flux and duration is programmable, triggered and monitored from a simple computer $RS232$ interface. It was tested to be reliable in ballooning temperature conditions: from $-80°C$ to $50°C$. Design and test's results are explained.

## 1 Introduction

High sensitivity far infrared and submillimeter camera in astrophysics plan to use (arrays of) bolometers. The Olimpo experiment, designed to measure the

[1] Corresponding author. Tel.: +33 1 69083625; e-mail: dyvon@cea.fr

Cosmic Microwave Background at high multipole moments (at high angular resolution), will use one bolometer array per frequency band at 4 frequencies (143, 217, 385 and 600 $GHz$). Infrared bolometers are extremely sensitive detectors, and their optical responses depend on the optical load and on the instrumental environment. Observers deal with the latter by calibrating the detection chain using standard sky infrared (IR) sources (primary calibration). Nevertheless, such a work tends to be time consuming, and instrument foregrounds and environment might change on time scales shorter than the time between two primary calibrations. Then a secondary calibration reference source is necessary. This is the purpose of the fast infrared calibration "lamp" hereafter named CalLamp. It was designed in the context of the Olimpo experiment, but it can be usefull in other high sensitivity experiments.

## 2 Goals and constraints on Callamp

In the Olimpo experiment the source is placed in front of a hole in a mirror cooled at 2 $K$ and fixed on it. When the source is heated by an electric impulse up to $20-25$ $K$ it will radiate, with a black body spectrum, during a time interval of a few hundreds millisecond. The CalLamp has three functional parts, each deposited on a common substrate: the black body radiative surface, a resistive heater and a thermometer.

In order to make the CalLamp a reference source, it has to be very stable. That means that, between "primary calibrations" the emitted light flux has to be reproducible to better than 1%, or that the temperature fluctuations must not exceed a few parts per thousand. So we decided to monitor the thermal behavior of the source with a thermometer placed on it. Stability is the first requirement. Here and in the following, stability means reproducibility.

The CalLamp is placed in a cold environment, carefully monitored by the cryogenics apparatus. Readout, command and monitoring electronics are placed outside the cryostat, in an hostile environment: the temperature of the atmosphere around a balloon ranges from $+60°C$ (Sunshine, ground) to $-80°C$ (transitory in flight), with typical working conditions of $-55°C \pm 10°C$. Every part of the source associated electronics were chosen for their low temperature dependence. Low temperature coefficient military components were used whenever possible.

Infrared bolometer main parameters are noise, thermal relaxation time, heat capacitance $C$, and thermal link $g$, all four being related. IR light pulse generated with rise time shorter than bolometer intrisic relaxation time allows to measure and test anomalous heat capacitance. Our goal was to achieve a risetime of 1 ms or less. Thus our design minimises heat capacitance.

The same lamp will be used to calibrate the four bolometer arrays. In laboratory, intercalibration of bolometers is a good test of optical behavior, and for this the optical spectrum of the lamp needs to be known.

## 3 The Design of the Calibration Source

Base design is the heritage of classical infrared bolometer design. The support is a thin monocrystal of synthetic sapphire, chosen for its mechanical strength, its large heat conductivity and its small heat capacity, dominated by phonon contribution (Debye's law). Calculations show that, at a few Kelvin the (Kapitza) thermal resistances drop fast and the computed thermal time constants for temperature relaxation within the active plate are below or of the order of 50 $\mu s$, smaller than the targeted rise time. Sapphire plate heat capacitance dominates all other contributions. As a compromise between mechanical strength and heat capacitance, we have chosen to use a 10x10x0.2 $mm^3$ sapphire plate. Heat leak to the source mechanical support (temperature reference at 2 $K$) is achieved through gold wires bonded on gold pads and on the brass mechanical holder.

The radiative surface is made of a thin metal layer deposited over this substrate. A heated metallic thin film, with impedance adapted to half the vacuum impedance (377 Ω) is known to show an emissivity of 50% and to emit a black-body spectrum. Very thin films deposits are delicate, and very sensitive to cracks and mechanical support surface quality. The choice of Bismuth, a semi-metal, solves this problem. The required thickness to achieve 188 Ω ranges from 90 nm to 150 nm, depending of the porousness of the deposit. This is what we chose to implement.

The heater is made of a thin resistive strip of Iridium, deposited on the other face of the sapphire substrate, a technology under control at CSNSM. This provides a low heat capacity heater, very stable with time. Heating time of 1 ms from 2K to 20K can be achieved under heating voltage as high as 18 volts, a large value in low noise cryogenic apparatus.

A large surface thin $Nb_xSi_{1-x}$ film thermometer (1) is deposited to monitor the temperature of the infrared source.
Except the $Bi$ film obtained from a crucible heated by Joule effect and in classical vacuum, all the components are evaporated in ultra-high vacuum by electron guns ($Ir$, $Au$ pads, $NbSi$). The $NbSi$ thermometric layer is obtained by co-deposition of $Nb$ and $Si$ under controlled rate to adjust the composition which governs the sensitivity at the suited temperature (here around 14 $K$). Special care is taken to improve the adhesion of the different films using thin

$Cr$ layers as sticking material for noble metals. A $SiO$ protection layer is deposited on the active parts of the device.

One of the source is shown in figure 1 and figure 2. On the first picture the two outer strips are the iridium deposit. The heating current flows in opposite direction in order to minimize the electromagnetic fields generated by it. The third strip from the border is a safe guard ring which is grounded in order to minimize the influence of the high currents in the iridium strip on the thermometer. The inner darker square is the thermometer. The Bismuth radiative layer is on the opposite face of the sapphire plate.

The source is completely shielded by a brass housing, except for a 5 $mm$ diameter hole in front of the Bismuth radiative layer. The sapphire plate is hold by small mechanical probes, one at each corner and each face. These probes have a spring inside to make the contact soft. In order to minimize the thermal leak, the contact between the sapphire plate and the probes are done with 1 $mm$ diameter sapphire balls glued on the probes. Cylindrical Delrain pins at each corner keep the source from moving in case of shocks

The electrical signals are carried through 15 $\mu m$ diameter, 7 $mm$ long brass wires to a printed circuit board (PCB). A 15 pin MDM connector is soldered on this PCB. Small diameter brass wires have been used to minimize the thermal leak towards the PCB, which is considered as a intermediate large thermal capacitance. A direct thermal leak to the bath is obtained using $25mm$ diameter gold wires bonded to the brass housing. All the wires were bonded using a wedge bonding machine.

After some trials, two sources were built and tested, in the following they are named "S1" and "S2".

## 4 Readout and Control-command electronics

### *4.1 Global design*

The functionalities of the readout and control electronics are shown in figure 3. More information is available in (2). The source thermometer resistance is calculated from the voltage $V_{th}$ measured when a polarisation voltage $V_{pol}$ is applied. The polarisation resistors $R_{pol}$ (200 $k\Omega$ $\pm 5\%$ each) have been selected for their very low temperature coefficient ($\frac{1}{R}\frac{dR}{dT} \simeq 5\ ppm/^{\circ}C$) (MSI resistors MSTF-2QN-2003j-DG). $V_{pol}$ is low enough not to heat the thermometer and bias the measurements. In order to get rid of offsets and low frequency noises, $V_{th}$ measurements are repeated with $V_{pol}$ reversed. High frequency noise

effects, are minimized by measuring $V_{th}$ several times ($N$) during the $+V_{pol}$ polarisation and during the $-V_{pol}$ phases. The resistance of the thermometer is calculated by taking the difference of the arithmetic averages of both series of $N$ measurements. Typical $V_{pol}$ values of 200 $mV$ and $N = 320$ during $20ms$ time intervals ensure good precision without heating the thermometer.

The heating impulse applied to the iridium strip has two parts (figure 10). A short high voltage part (typically 14 $V, 10$ $ms$) in order to reach the nominal temperature ($\geq 20$ $K$) as quickly as possible, followed by a plateau (typically $\simeq 7$ $V, 200$ $ms$) to stabilize the source temperature. The source temperature and bolometer responses are measured during this second phase.

All the above parameters are sent, through a $RS232$ link, to a microcontroller (MC) situated on the electronic board. We use the very convenient Pic16F877-20I/P device from Microchip Technology Inc. that provides an RS232 interface to the balloon data acquisition computer, and 5 I/O digital ports used to drive and read the several DAC and ADC of this board.

The heating signal is generated by a three positions switch commuting the output to several voltages. The high and the low voltages are generated by a digital to analog converter (DAC) commanded by the MC. The signal is sent to the iridium strip through a follower and an inverting amplifier to achieve symetric polarisation.

The thermometer readout system is shown in figure 4. The polarisation voltage, generated by a DAC, is reversed by varying a switch position between $0V$, $+V_{pol}$ and $-V_{pol}$ The MC pilots the switch position and the DAC value. The $V_{th}(t)$ signal is amplified by a low noise differential amplifier, followed by a second order low pass filter and an ADC. Since after the low pass filter the signal needs a certain time to stabilize, $N$ can not be increased too much.

We found that the source temperature never reaches a true plateau (see section 5), thus the measurement cycle is repeated three times during the second phase of the heating. The MC calculates and delivers one thermometer resistance per measurement cycle.

### *4.2 The readout preamplifier*

Assuming a typical thermometer impedance of 100 $k\Omega$ at a temperature of 20 K, we compute a Johnson noise of 3.3 nV/$\sqrt{Hz}$ and 33 fA/$\sqrt{Hz}$. We request the preamplifier noise to be negligible in the noise budget. Signal bandwidth is small: requiring to be able to monitor a risetime of 0.1 ms leads to a cutting frequency of 3 kHz. These constraints are met by designing a bolometer JFET preamplifier. JFETs do not need to be cooled, given the

quite low thermometer impedance. We designed a board (see figure 5) that can be seen as a very simplified version of the one described in (3) . We use a differential voltage preamplifier, optimised for low noise at low frequencies. Front end transistors are the classical 2SK146 JFET matched pair followed by a cascode circuit implemented using a matched bipolar pair. The AD8620 dual JFET Operational Amplifiers run within a transimpedance circuit with 1 $M\Omega$ feedback, combined with the large JFET transconductance, allow open-loop gain larger than $10^4$ with excellent stability criteria. Close-loop gain of the first stage differential amplifier is 40. Great care was taken to filter noise coming from power supplies. Finally, the preamplifier DC offset is measured using an integrator circuit that connect to point A, and cancels for small JFETs' asymmetry. Second stage is a classical JFET differential amplifier with gain 5. We measured a flat noise level of 2 $nV/\sqrt{Hz}$ and a 1/f knee frequency of 20 $Hz$.

### *4.3 Interface with data acquisition*

The microcontroller is driven by a serial RS232 interface. The on board balloon computer uses a C library to parametrise, trigger the light pulse and recover the monitoring thermometer resistance values. Heating pulse (Voltage, length) and thermometer readout parameters are fully configured from the on board computer. Thermometer readout parameters include thermometer polarisation voltage and length, number of averaged measurements on polarisation polarities, number and delay of polarisation cycles. When the on board computer triggers the CalLamp, after a delay, the board returns the three monitoring thermometer resistance values.

### *4.4 Laboratory tests and performances*

The measurement precision is a direct consequence of the high frequency electronic noise, and in the following we distinguish this from stability measurements. The first means the standard deviation for measurements repeated in short time intervals (few minutes), while the second concerns variations over several hours or day time scales. Both were studied using 10 $k\Omega$ temperature independent resistors.

With 600 $pW$ of total sensor dissipation injected during 40 $ms$, the measurement standard deviation achieved for the resistive value of a 10 $k\Omega$ thermometer reaches 0.5 $\Omega$ (48 $ppm$), at a stabilized temperature. The corresponding uncertainty on the source source temperature measurement is $\frac{\delta T}{T} \simeq 2\,10^{-5}$ . and is negligible with respect to the requirement.

The stability of the readout electronics and polarisation voltage generator with respect to external temperature was checked by putting the electronics in a thermal box whose temperature could be adjusted precisely. It was varied between 20 $°C$ and $-60$ $°C$ by steps. Two electronic boards were tested giving $\delta R = 60\Omega$ for the 80 $°C$ range, which corresponds to an error on the source thermometer temperature measurement of $\frac{\delta T}{T} \simeq 3\ 10^{-5}/°C$ at $T \simeq 25\ K$ for both sources.

## 5 Calibration source performances

### *5.1 Experimental setup for source caracterisation.*

In order to measure their thermal and stability properties, the sources were fixed on the copper tank of a liquid He cryostat, and the temperature of this "thermal bath" was repeatedely measured with calibrated resistive temperature probes. The copper tank temperature was 4.4 $K$ and could be lowered down to $\simeq$ 2.5 $K$ by pumping. It was stable within a few hundredth of a $Kelvin$.

All the signals (polarisation, heating, resistance measurement) were carried through very low noise cryogenic cables identical to those which will be used in the experiment.

### *5.2 Source thermal behaviour.*

We first recall quickly the required source properties for the Olimpo experiment. At rest the source temperature $T_0$ will be 2 $K$. When heated, the working temperature $T$ ($\sim$ 25 $K$), has to be as constant as possible during light emission. The rise time must be short ($\sim$ 1 $ms$) in order to be able to measure the telescope bolometer time constants, and the recovery time to $T_0$ should not introduce unwanted dead time. The power dissipation has to be small, and the radiation emission has to be more stable than 0.5 % over several days.

Let us consider the simplest thermal model for the source (left diagram of figure 6) with one calorific capacitance $C$ representing the sapphire and its coatings, and one leak $g$ to the bath at $T_0$. If $C$ and $g$ were independent of the temperature, which is not true, the transition time would be given by $\tau = C/g$ and, for a constant electric power $W$ dissipated in the iridium strip, the asymptotic temperature would be $W/g$.

A temperature fast rise time requires a low thermal capacitance and a large thermal leak. Mechanical considerations forbid very thin sapphire plates ($\lesssim$ 100 $\mu m$). Thus a compromise had to be done and sapphire thickness was chosen to be $\simeq 200\ \mu m$. With a large thermal leak, the electric power needed to achieve a given temperature ($20 - 30\ K$) should be high and could damage the thin iridium strip. Therefore the design has been a compromise between the requirements.

In order to optimise the source properties and to understand its behaviour, a full thermal caracterisation has been performed.

First the relation between the source thermometer resistance $R_{th}$ and the sapphire temperature has been measured. To do that, the source was fixed on a plate whose temperature was adjustable and measured. Figure 7 shows the measurements for the two sources. These results are reasonably described by functions of the type $R_{th} = R_0 \exp((\frac{\Delta}{T})^{\delta})$ with $\delta = 0.244$ for source $S1$ and $\delta = 0.313$ for source $S2$.
As we shall see later, the diagram of figure 6a does not allow to reproduce the source thermal behaviour, and we will need the two stage thermal modelisation of figure 6b. In that figure, $g$ represents the direct leak to the bath, for instance through the gold wires linking the sapphire to the brass housing. $C_2$ represents the intermediate parts (PCB, fixation probes). Because their thermal capacitances and leaks are unknown functions of the temperature (not even linear), this simple schema is too complicated to use. It can be simplified and linearised by considering very small square electric impulses to heat the iridium strip. The thermal homogeneisation time of the sapphire plate is assumed to be negligible. We assume also that $C_2 \gg C$. With these measurement conditions and assumptions, the two stage diagram reduces to the simpler left schema ($T_2 = T_0 = Cte$), with $g \equiv g + g_1$.

The method is illustrated in figure 8 which shows the preamplifier output for the source $S1$, whose rest temperature is $T_0 \simeq 4.4\ K$, heated by a 35 $ms$ long electric impulse of 23 $mV$. The black curves represent two separate exponential fits. The two caracteristic decay times, which are very consistent, provide $C/g$.

From this and the asymptotic temperature we deduce $g(T_0)$ and $C(T_0)$. By varying $T_0$ as described above, we obtained the results shown in figures 9. These functions are well reproduced by $C \approx T^{\alpha}$ and $g \approx T^{\beta}$, where $\alpha \simeq 3$, and $g \simeq 2$.

When used as a calibration lamp, the source is heated by electric impulses like the one in figure 10. The first part heats the source very quickly, and the second part keeps the temperature as constant as possible. Figure 11 shows the temperature response to the typical impulse of figure 10. Please, note that the large measurement dispersion on the temperature plateau is only due to

the fact that a very low polarisation current was used in order to get the whole impulse shape, without saturating the preamplifier at low temperature, where the thermometer resistance is high. This figure is not representative of the normal working conditions. The simplest thermal diagram cannot explain the shape of the temperature fall. Using the results described above, the main features of the signal can be reproduced by a simulation based on the second schema, although there are many unknown functions. One of the main consequence of the parasitic capacitance $C_2$, is that it is almost impossible to find a set of electric parameters allowing a constant source temperature. Therefore, the thermometer resistance is measured at three equidistant places during the electric plateau.

One can ask which part of the design play the role of $C_2$. By removing two out of the four fixation "probes", the measurements of the leak and of the thermal capacitance, as described above, have shown that these mechanical parts represents about half of the undesired additional thermal capacitance $C_2$. In order to minimise the contribution of the PCB, the source was connected to it by 15 $\mu m$ diameter brass wires instead of gold wires. The thermal leak to the brass housing was increased by adding a gold wire. The gain on the total relaxation time was small (about 0.5 $s$ for a total approximate time of 3 $s$). The parasitic capacitance could perhaps be lowered by improving the mechanical fixation.

The thermometer resistance is measured at 3 fixed times after the beginning of the electric heating impulse. The polarisation value is chosen high enough (200 $mV$ for source $S1$ and 400 $mV$ for $S2$) in order to minimise the measurement errors but without risking to saturate the preamplifier output. The typical resistance measurement noise was $\simeq$ 1 $\Omega$ for a resistance value of $\simeq$ 17500 $\Omega$ at 25 $K$ for the source $S1$, and $\simeq$ 5900 $\Omega$ for the source S2. The corresponding error on the temperature is completly negligible ($\delta T/T \simeq 10^{-4}$ for the source $S2$).

### *5.3 Stability measurements.*

In order to check the stability of the sources, one should measure their radiation fluxes over a period of the order of the experiment duration, and correlate them to their temperatures deduced from their thermometer resistances. In practice, it is necessary to use bolometers to measure the flux, but we had none. We have proceeded as described hereafter for both sources simultaneously.

Stability checks were performed for both sources, using heating electric impulse similar to the one of figure 10, over several periods of several days each. The

source working temperature was $\simeq 25\ K$.

The electronics (preamplifier, power supply) was at room temperature. Temperature probes have been put inside the preamplifier boxes. We have checked that the source temperature measurement is insensitive to any variation of power supply output within $\pm 1\ V$. Using fixed resistors with very low temperature dependence ($1 ppm/^\circ C$) we checked the excellent stability of the readout part with respect to electronic temperature variations (see section 4).

The dependence of the source temperature relative to the bath one ($T_0 \simeq 4.4\ K$) has been measured by changing $T_0$ by a few tenth of Kelvin. The result is $\delta R(T)/\delta T_0 = -40\ \Omega/K$ for the source $S1$ and $-9\ \Omega/K$ for the source $S2$, for $T \simeq 25\ K$. This is in agreement with the fact that the thermal capacitance is a rapidly increasing function of the temperature (figure 9). The variations of $T_0$ are small enough (a few hundredth of $K$) and this effect is totally negligible.

We observed a residual variation of the thermometer resistance with the electronic temperature, which is due to the temperature dependance of the heating pulse generator (DAC). When stabilised to better than $\pm 0.5^\circ\ C$ almost no variation was observed. Therefore DAC instabilites lead to real temperature variations of the source that we will have to correct for using the source thermometer information. If we call $T_{ext}$ the temperature of the electronics, these residual variations amount to: $\frac{\delta R}{\delta T_{ext}} \simeq 10\ \Omega/^\circ C$ for the source S1, and $\simeq 2\Omega/^\circ C$ for for the source S2 at 20 $^\circ C$. This means respectively: $\frac{\delta T}{T} \simeq 2.4\ 10^{-4}\ /^\circ C$ and $\frac{\delta T}{T} \simeq 1.4\ 10^{-4}\ /^\circ C$ at 20 $^\circ C$.

Figure 12 shows the temperature fluctuations measurement decorrelated from the electronics temperature variations for a four day period. With $\frac{\delta T}{T} \lesssim 10^{-4}$ the stability is within the requirements.

### *5.4 Emissivity measurements*

A cryogenic bolometer at 2K was used as a radiometer to measure the total power emitted by the CalLamp. A Winston cone (4) collects the rays with an angle of incidence below $\theta_{max} = 15.5^\circ$. The bolometer is close enough to collect all the rays emitted by the source within this angle. Thus, the total power absorbed by the detector is given by the following relation :

$$P_R = \eta\ A_S\ \epsilon\ L_{bb}\ \pi\ sin^2\theta_{max}$$

Where $\eta$ is the detector optical efficiency, $A_S$ the source aperture surface ($m^2$),

$\epsilon$ is the surface emissivity and $L_{bb}$ the surface blackbody radiance ($W/m^2/sr$).

By using a lock-in technique, we have measured the electrical response of the bolometer to a variation of the source temperature. We define the voltage response of the bolometer :

$$S_V = \frac{\Delta V}{\Delta P_R} = \frac{1}{\eta\ \epsilon}\ \frac{1}{A_S\ \pi\ \sin^2\theta_{max}}\ \frac{\Delta V}{\Delta L_{bb}}$$

$\Delta V$ is the voltage variation and $\Delta L_{bb}$ is the variation of the blackbody radiance for the imposed temperature variation. The product $\eta\ \epsilon\ S_V$ can be calculated from the measurements. In a first step, we used a homemade blackbody source ($\epsilon = 1$) whose temperature was varied from 15.7 to 19 $K$. The product $\eta S_V$ obtained is constant and estimated to $546 \pm 11\ 10^3\ V/W$. The blackbody source was then replaced by the calibration lamp. The source temperature was varied between 8.5 and 28K, and the product $\eta\epsilon S_V$ obtained was $155 \pm 4\ 10^3\ V/W$. Thus the mean emissivity of the calibration lamp within the measurement solid angle is estimated to be $28 \pm 4\%$.

## 6 Conclusion

We made and extensively tested a calibration Lamp for Submillimeter and IR bolometers experiments. This device is designed to be operated at liquid Helium temperature. It features millisecond risetime, and excellent reproducibility of light pulse. A small instability correlated to the driving electronic temperature of the heater is nevertheless observed, but we showed that the Cold plate monitoring thermometer allows efficient decorelation of this effect. Future improvement will allow to get rid of this problem. The board has been tested in environnements representative of the stratospheric balloon flights and proved excellent behavior. All operating parameters can be configured through the data acquisition computer. We believe that this device will be a usefull tool as a calibration lamp for observations, but also as a tool for caracterising the optical behavior of any infrared bolometer device.

## 7 Acknowledgments

The authors would like to thank the Bureau d'Etudes of DAPNIA, especially D.Leboeuf and G.Coulloux, in designing the mechanical holder of the CalLamp. We are also grateful to S.Herve and J.Labbe for their valuable help and assistance, respectively in wire bonding and cable soldering.

## References


[1] S.Marnieros, "Couches minces d'isolant d'Anderson. Applications à la bolométrie à très basse température", Thèse de l'Université de Paris XI (1998).

[2] M.Fesquet et al., IEEE Nuclear Science Symposium Conference Record (2005) N14-26.

[3] D.V. Camin et al., Alta frequenza 56 (1987) 347.

[4] R.Winston, J. Opt. Soc. Am., 60, 2 (1970) 245-247.

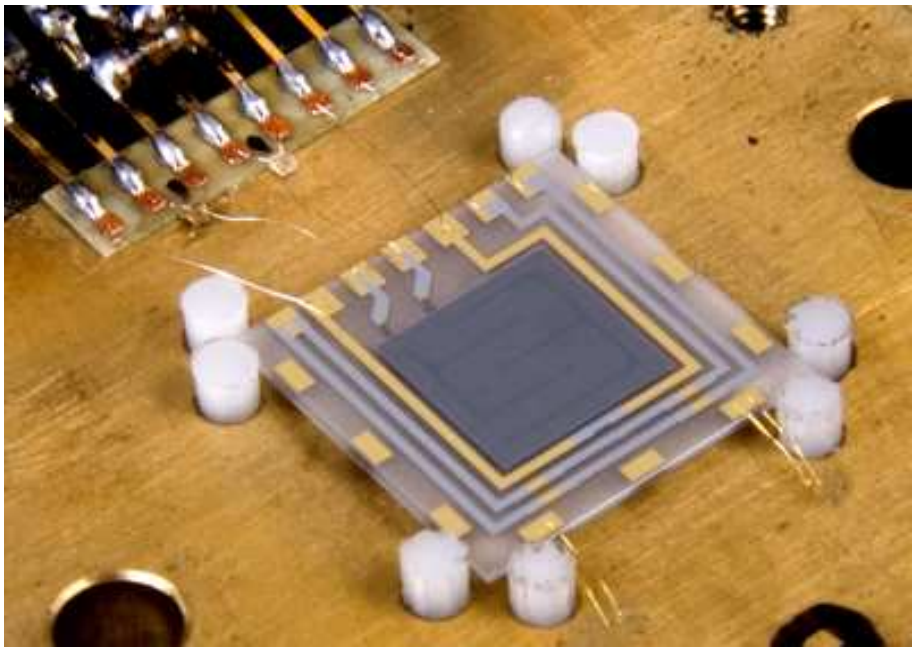

Figure 1. Source view showing the thermometer (dark central square) and the iridium heating strip. The Bismuth layer is on the opposite face and not visible here.

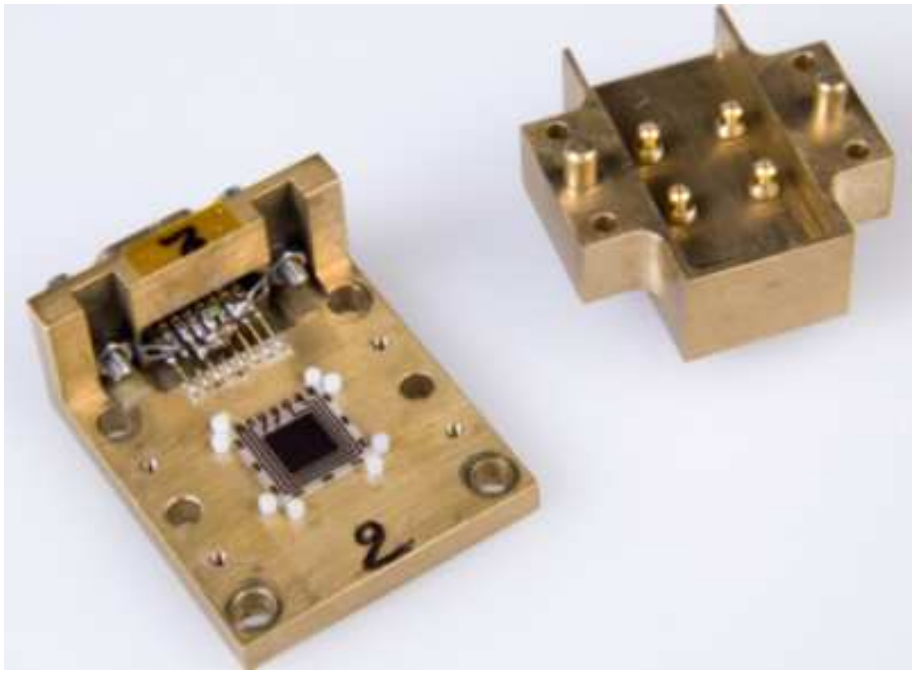


Figure 2. Source mechanical housing.

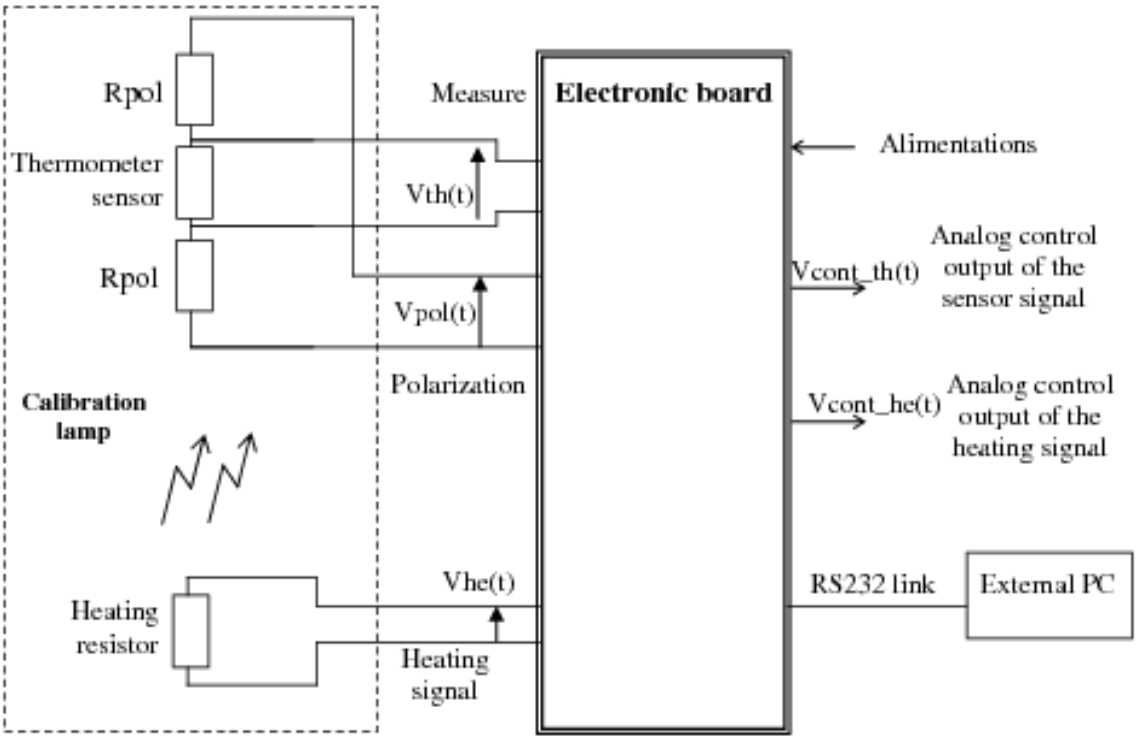


Figure 3. Electronic functionalities.

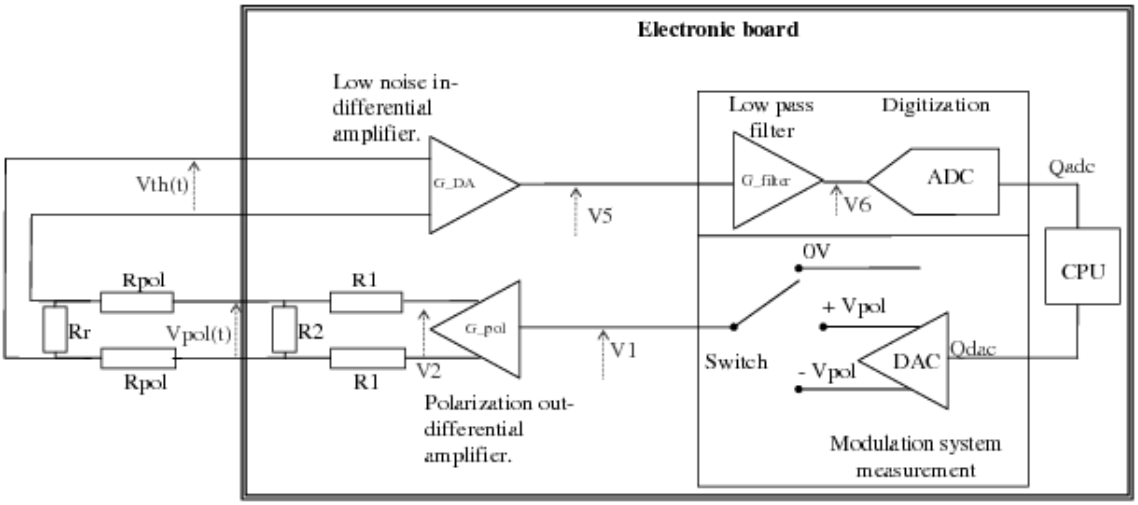


Figure 4. Readout electronics.

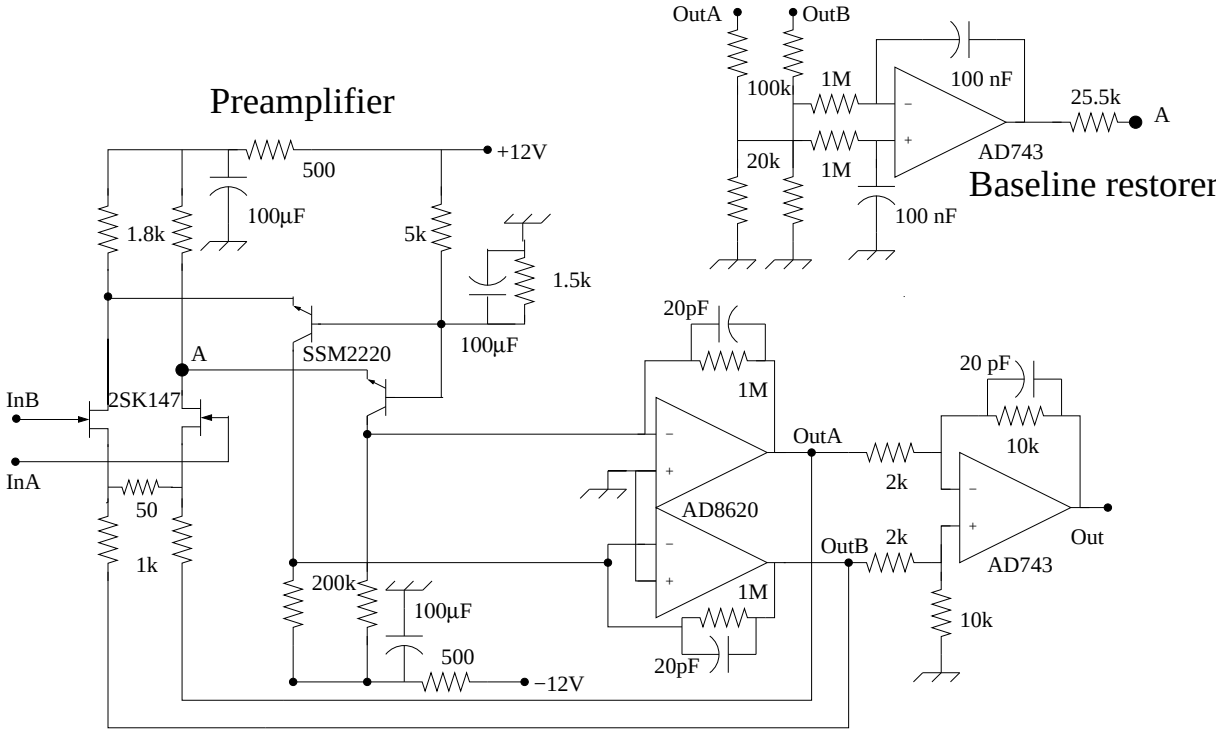


Figure 5. Design of the readout preamplifier.

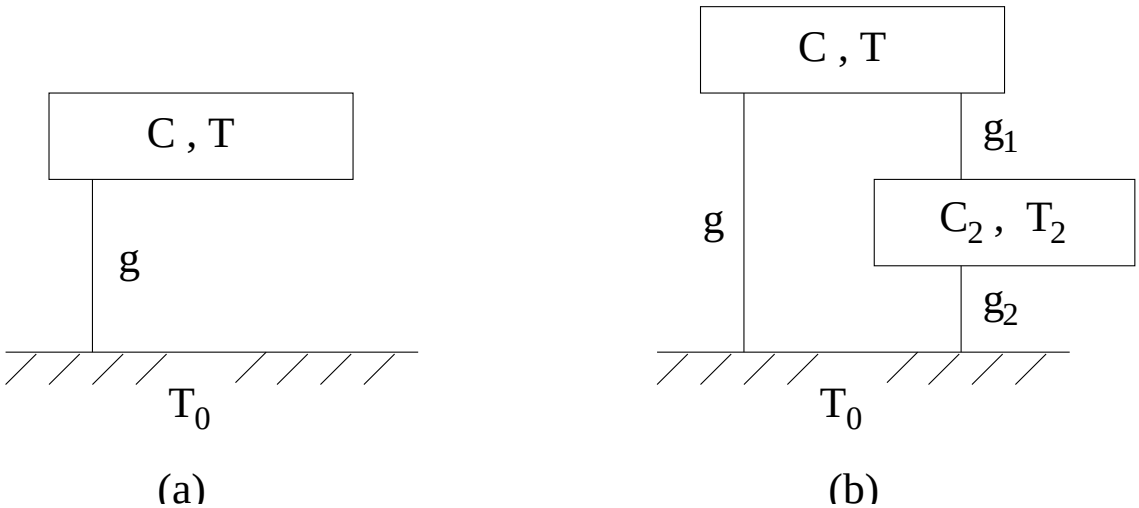


Figure 6. Thermic diagrams.

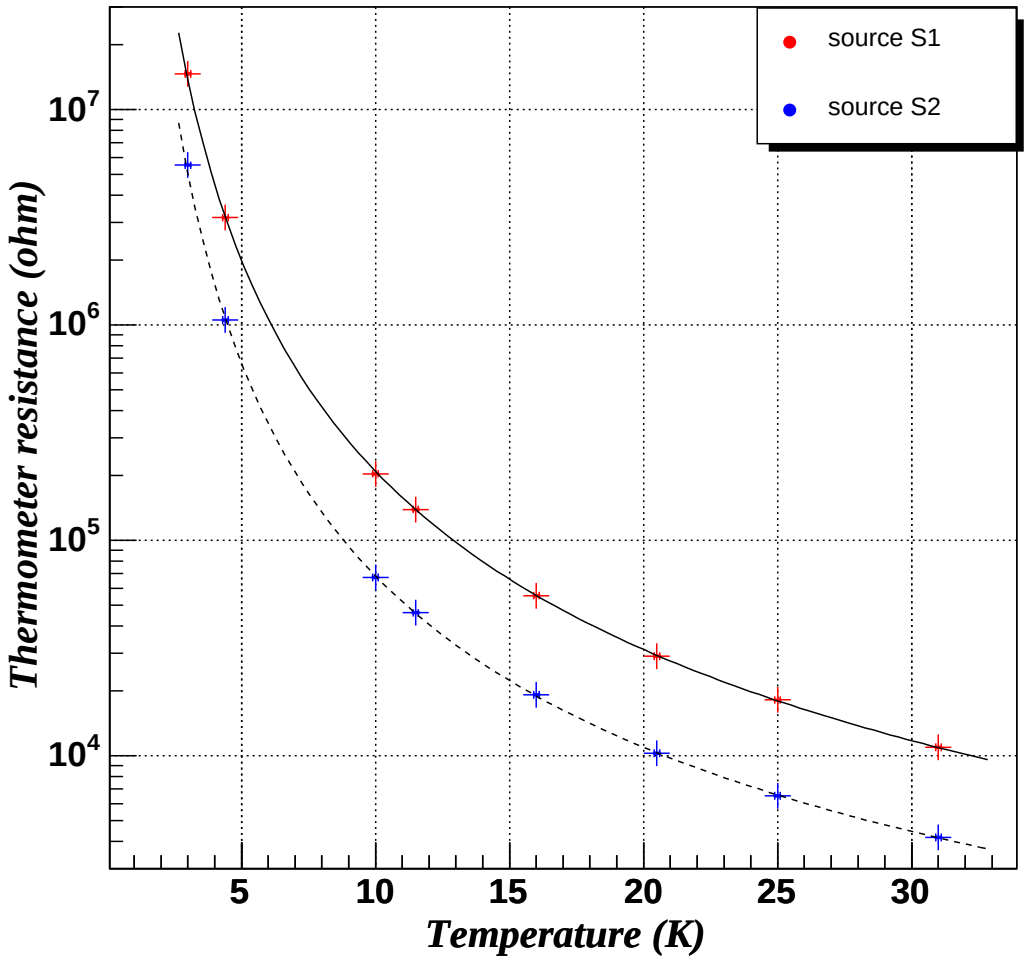


Figure 7. Thermometer resistance as a function of temperature.

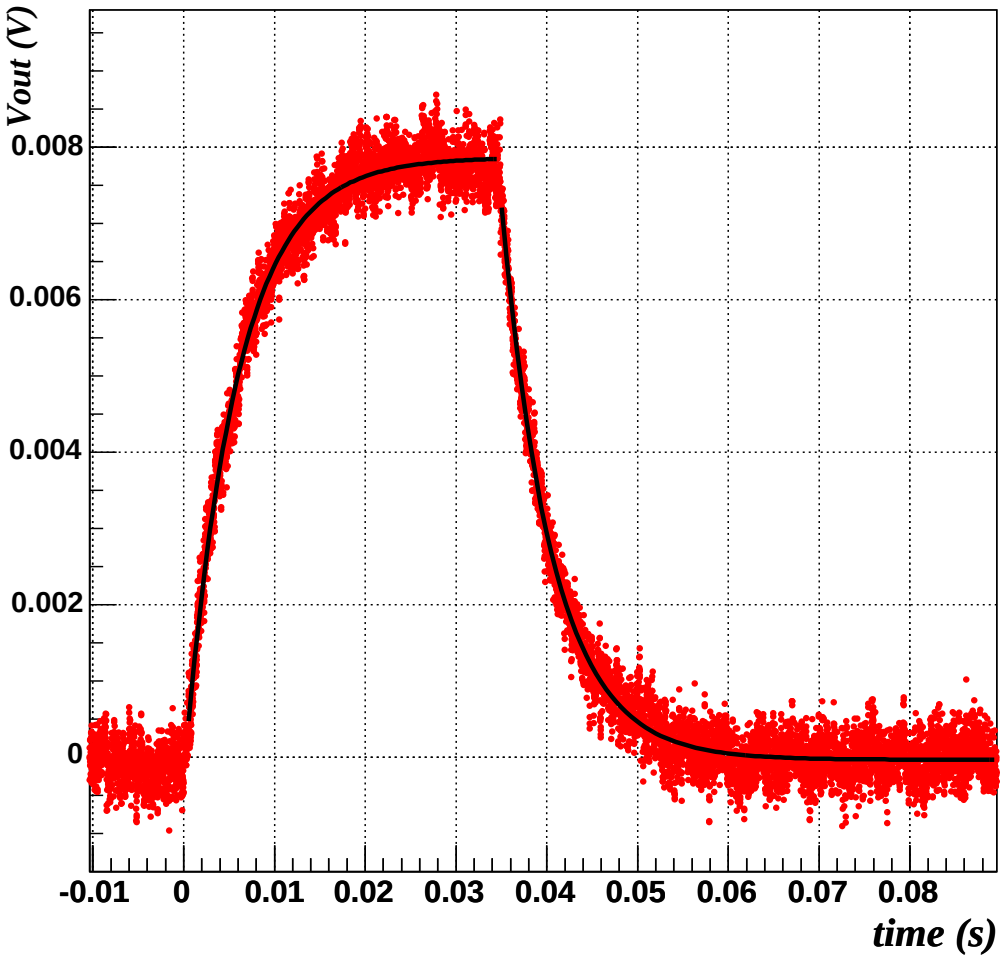


Figure 8. Preamplifier output versus time for small heating impulse.

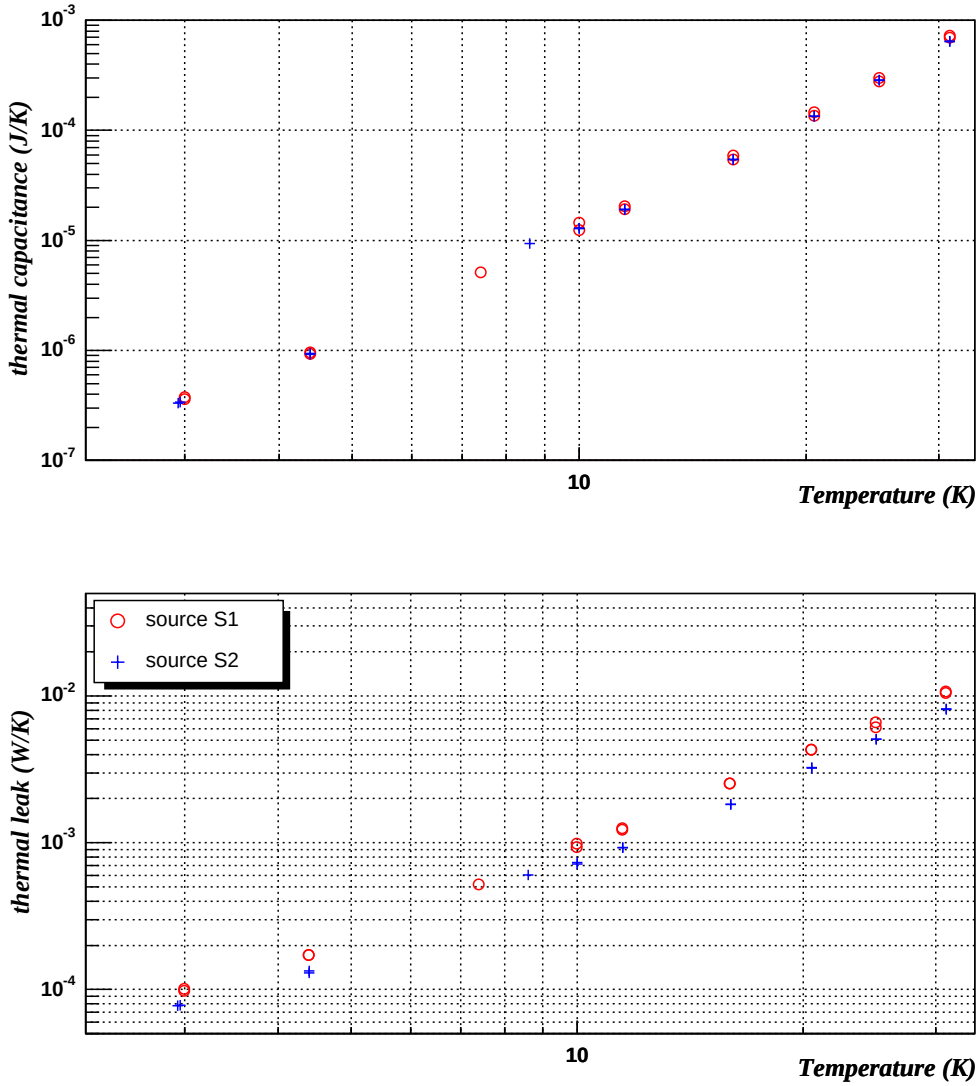


Figure 9. Temperature dependence of thermal capacitances and thermal leaks.

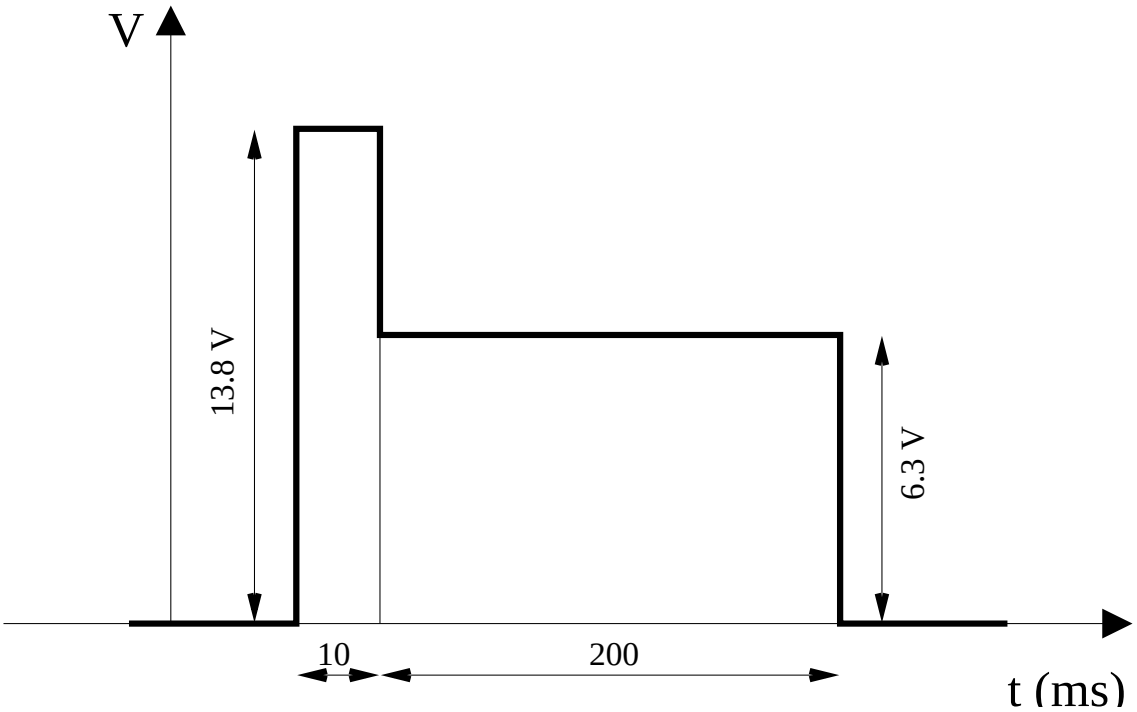


Figure 10. Exemple of heating impulse.

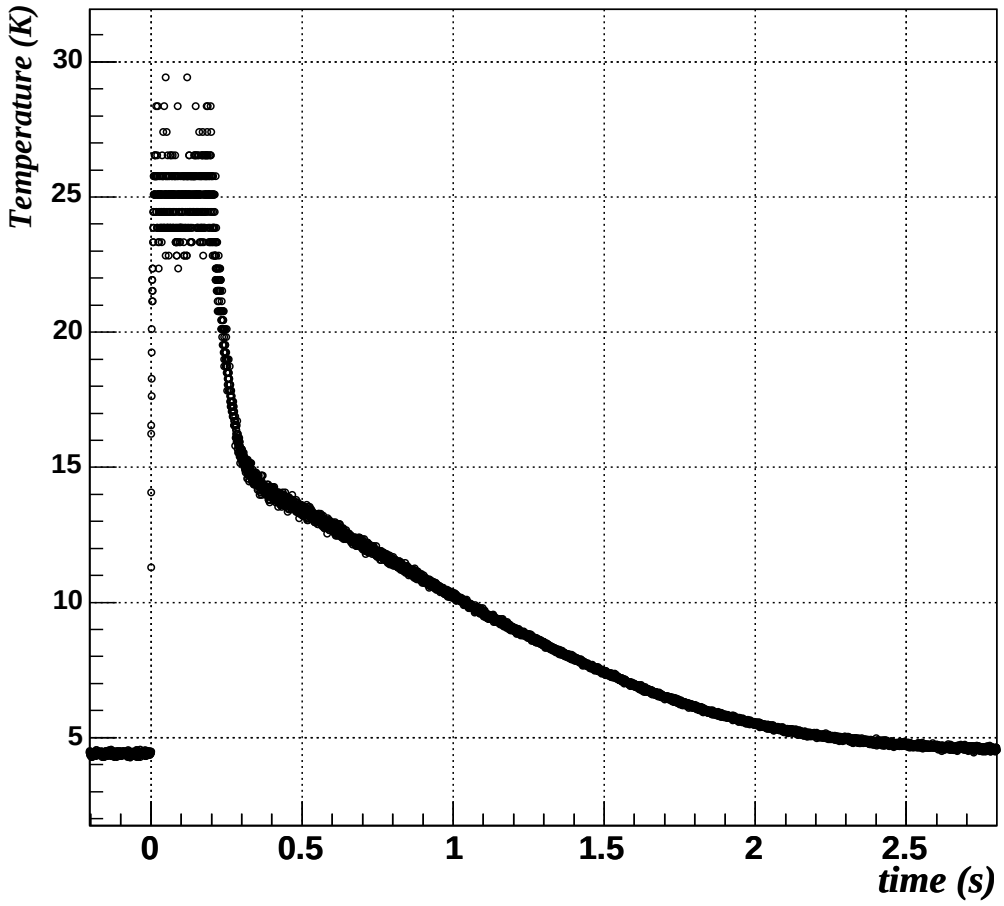


Figure 11. Preamplifier output versus time for standard heating impulse.

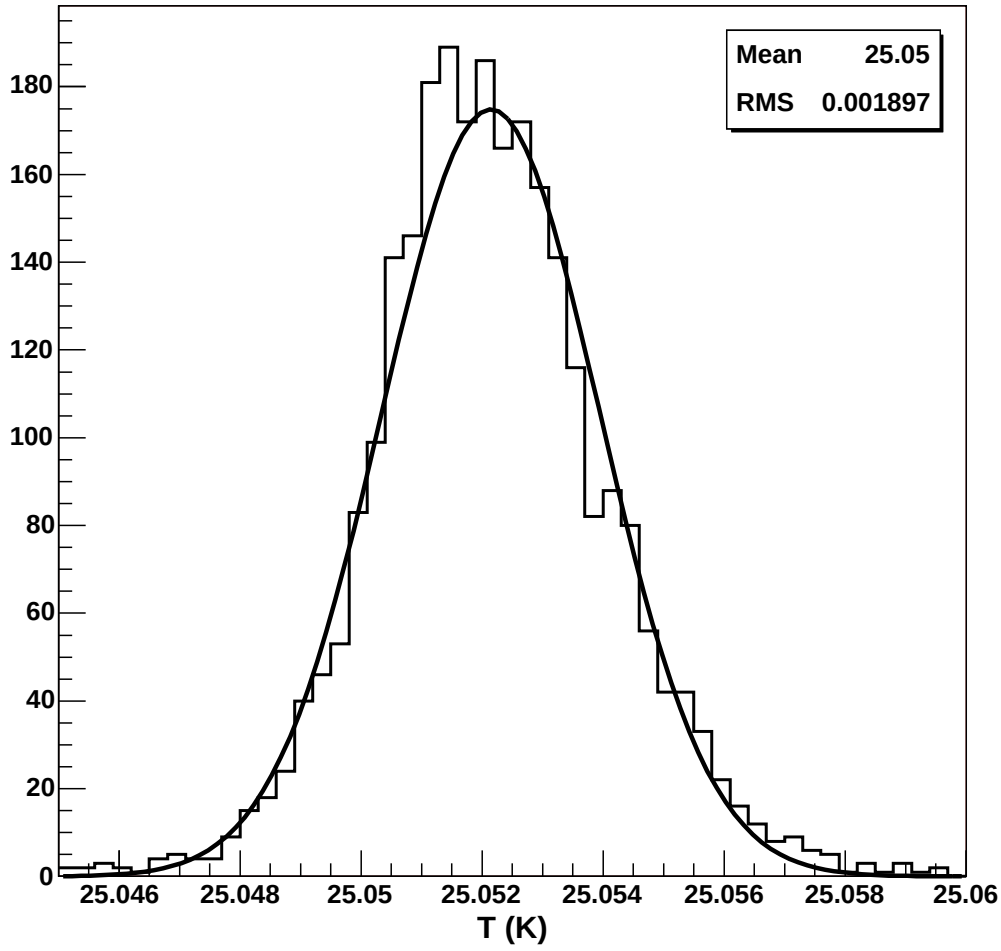


Figure 12. Source temperature measurement distribution decorrelated from electronics temperature corresponding to a three day period.